European Journal of Agronomy 134 (2022) 126460

Contents lists available at ScienceDirect

European Journal of Agronomy

journal homepage: www.elsevier.com/locate/eja

Water and carbon fluxes in an apple orchard during heat waves

D. Zanotelli [a,*], L. Montagnani [a,b], C. Andreotti [a], M. Tagliavini [a]

[a] Faculty of Science and Technology, Free University of Bolzano-Bozen, Piazza Università 5, 39100 Bolzano, Italy
[b] Forest Service, Autonomous Province of Bolzano-Bozen, via Brennero 6, 39100 Bolzano, Italy

ARTICLE INFO

Keywords:
Climate change
Evapotranspiration
Fruit trees
Heat stress
Net ecosystem exchange
Primary productivity

ABSTRACT

Prolonged hot periods known as heat waves (HW) are likely to increase in frequency and intensity due to climate change. Several studies analyzed the impact of recent heat waves on different un-managed terrestrial ecosystems, while little is known about the change they provoke in the carbon and water fluxes on irrigated agroecosystems. In this study we analyzed observations from 6 years continuous eddy covariance measurements (2013–2018) in an apple orchard located in South Tyrol (Northern Italy), regularly irrigated to prevent any limitations in soil water availability. The aim was to assess the impact of the heatwaves (at least 3 consecutive days of unusually high maximum temperature for the summer period) on the gross primary production (GPP), net ecosystem exchange (NEE), and actual evapotranspiration (ETa) fluxes. Out of the 13 heat waves that emerged from the temperature data analysis, five occurred in 2015, which together with 2013 was the hottest year in the considered period. In these two years, GPP and NEE patterns indicated a small but significant reduction in the assimilation capacity of the orchard with increasing T_{max}, which was not present in the remaining years. ETa, instead, consistently increased across all the temperature range. During heatwaves, we observed an increase in the available energy, and a further reduction in the sensible heat flux in favour of latent heat, with a consequent increase in ETa. Additionally, during 9 out of the 13 heat waves, ETa values were among the 5% highest ever recorded in summer. Although heatwaves differed in length (max. 8 days) and magnitude (with peaks of 37 °C), ETa generally increased during heat waves by approximately 9% with respect to the week before. No similar consistent patterns were observed for GPP and NEE, which supports the hypothesis of decoupling between carbon and water fluxes during heat waves in an irrigated agroecosystem.

1. Introduction

The increase of greenhouse gas concentrations in the atmosphere is likely to enhance both the intensity and the frequency of future extreme climate events, like heat waves (HW) (Frank et al., 2015; Perkins, 2015). Heat waves are unusually hot periods for the season they occur, lasting around a week or less, although sometimes they can stretch longer (Von Buttlar et al., 2018). The effects of heat waves are especially severe in summer because they are associated with extremely high air temperatures, as in the recent example July 2019 in several European Countries (Sousa et al., 2020). Their occurrence is related to the presence of anticyclones, stationary systems with a center of anomalously high pressure on the same location for long periods (Perkins, 2015).

Heat waves are expected to impact the carbon and water balances of terrestrial ecosystems (Frank et al., 2015; Wang et al., 2016). If adequate water is provided to the ecosystem during heat waves, both transpiration and evaporation have the potential to increase as available energy and temperature increase, but this does not happen in the same way in the different vegetation types. Tree and grass systems show a distinct transpiration behavior during heatwaves: while the grasses tend to release all the available water until their desiccation, forest trees tend to close the stomata, therefore preserving soil water and the functionality of their wood vessels (Teuling et al., 2010). It has not been described yet if and to which extent, irrigated fruit trees under heat waves close the stomata, therefore enhancing the sensible heat release, or increase the latent heat flux (De Kauwe et al., 2019). Plant species exposed to excessive hot temperature as compared to its optimum, tend to decrease the net photosynthesis and the gross primary production (GPP) (Teskey et al., 2015; Wohlfahrt and Gu, 2015). For example, forests showed 30–50% less GPP during the heat wave hitting Europe and Russia in summer 2003 and 2010 (Bastos et al., 2014; Ciais et al., 2005). Leaf photosynthetic rate in apple trees, similarly also to other C_3 perennial species, reaches its maximum around 25–30 °C (Greer, 2015a) and the entire photosynthetic apparatus can be severely compromised if

* Corresponding author.
E-mail address: damiano.zanotelli@unibz.it (D. Zanotelli).

https://doi.org/10.1016/j.eja.2022.126460
Received 30 March 2021; Received in revised form 1 January 2022; Accepted 6 January 2022

extremely high temperatures occur. Heat waves characterized by maximal temperatures above 40 °C for periods lasting 4–7 days permanently reduced photosynthesis of apple leaves (cv. Red Gala) in southeastern Australia (Greer, 2015a, 2015b). The reduction of the assimilation during the heat waves is the result of both stomatal and non-stomatal limitation. Stomatal conductance (gs) at temperatures higher than 40 °C was only half of that recorded at 25 °C (Greer, 2015b). Moreover, both the enzymatic carboxylation and the regeneration of the carboxylating substrate ribulose 1,5-bisphosphate (RuBP) were strongly limited by high temperatures (Greer, 2015b). Besides the negative effects on the photosynthetic performances, heat waves may also severely impair apple fruits quality and cause sunburn, fruit browning and necrosis damages (Felicetti and Schrader, 2008). How these events influence the repartition of the available energy into sensible and latent heat as well as the net and gross carbon fluxes of the agro-ecosystems, is still largely unknown.

The net ecosystem exchange (NEE) is the result of the net CO_2 exchange between the ecosystem and the atmosphere, due to photosynthetic carbon assimilation (Pn) at the one hand and the respiratory carbon releases at the other hand, and accounts for the ability of an ecosystem to temporarily accumulate (negative sign) or loose (positive sign) carbon (Chapin et al., 2006). If soil water availability is not limiting, ecosystem respiration, contrary to Pn, increases because of increased soil temperatures (Lloyd and Taylor, 1994; Scandellari et al., 2015), a fact that might lead to a shift of the system from C sink to C source (Allen et al., 2005).

Most of the published literature about heat waves refers to natural and forest ecosystems, where heat waves occurrence is often accompanied by severe reductions of soil moisture. To which extent such behavior also holds true for irrigated agricultural systems, where heat waves occur in the presence of adequate soil moisture, is still unknown. Irrigation has a two-fold effect on plants: on the one hand, it provides water to the plant, reduces the risk of xylem embolism, and allow stomata opening. On the other hand, it reduces the peaks in temperature (Solomakhin and Blanke, 2010). These combined effects can enhance photosynthesis, but at the cost of an enhanced transpiration (Li et al., 2021; Teskey et al., 2015; Thiery et al., 2020).

In this paper we analyzed the effect of maximum daily summer temperatures on ETa (actual evapotranspiration), NEE and GPP, and we hypothesized that ETa increases, NEE become less negative and GPP decreases during heat waves periods. Additionally, we tested the hypothesis that the way ETa, NEE and GPP response during the heat wave period depends on gradualness of the temperature (T) increase as well as on the T_{max} values in the period before the onset of the heat wave.

2. Material and methods

2.1. The study site

The experimental site was a commercial apple orchard located in the municipality of Caldaro (46°21' N, 11°16' E, 240 m a.s.l.), at the bottom of the Adige Valley (North Italy), within an apple growing district. Apple (*Malus x domestica*, Borkh.) trees of the Fuji cultivar grafted on the dwarfing rootstock M9 were planted in 1999 in rows at a distance of 1 m along the row and 3 m between rows. The canopy size was kept constant over the years by winter pruning. The training system was slender spindle and the seasonal variability of tree height ranged between approximately 3.5 m after pruning to 4 m at the end of the season. The soil in the upper 0–60 cm layer was classified as loamy according to the USDA classification. Maximum soil water holding capacity assessed experimentally was 0.37 m^3 m^{-3} (Zanotelli et al., 2019), while the permanent wilting point, according to soil texture was set at 0.12 m^3 m^{-3}. The water table, controlled by a drainage system, ranged for most of the time between 1.20 and 1.85 m depth (Montagnani et al., 2018). Average yearly precipitation during the measurement period (average 2013–18) was 860 mm. Additional information on the annual pattern of temperature, rainfall, vapor pressure deficit (VPD) and global radiation (Rg) is present in Fig. S1. The orchard was provided with a drip irrigation system. In addition, in early spring, to prevent frost damages, and occasionally in summer, the site was irrigated by overhead sprinklers as well. Soil water content was continuously measured by means of 3 TDR probes (CS616, Campbell Scientific, Inc., USA) inserted vertically in the soil so to get an integrated value of the first 30 cm of the soil layer. The measurements were interrupted in autumn 2017 due to instrument failure, a problem that persisted for the whole 2018 year. Soil pH (in water) ranged from 7.2 (in the upper 0–20 cm soil layer) to 7.6 (between 40 and 60 cm soil depth). Orchard management was carried out according to organic farming guidelines. Average fruit yields in the considered period were in line with those of the local production area and above 60 t ha^{-1} (Zanotelli et al., 2019). Details on net ecosystem carbon balance and ETa pattern can be found in Zanotelli et al., (2015, 2019).

2.2. Measurements of ETa, NEE and GPP

NEE and ETa were measured by the eddy covariance (EC) technique from 2013 to 2018. EC instrumentation consisted of a sonic anemometer Gill R3, Lymington, UK and by a Li7200 CO_2/H_2O infrared gas analyzer (LiCor Biosciences, US, LiCor henceforth), mounted horizontally without filtering at 1.5 m distance from the air intake. Both instruments were mounted at 8 m height on a tower located inside the orchard (Zanotelli et al., 2013). The footprint area of the measurement tower, using daytime summer data, confirmed that the fluxes were originated by apple orchards, apart from headlands and farms roads (Fig. S2). Turbulent flux measurements (vertical wind velocity and CO_2 and H_2O concentration) were taken at 20 Hz and raw flux data were performed using EDDYSOFT software (Kolle and Rebmann, 2007; Mauder et al., 2018) every 30 min as described in Zanotelli et al. (2013).

The site, perfectly flat but surrounded by mountains, was subject to conditions of lack of stationarity and poor turbulence, particularly frequent in winter and at night. Consistently with previous works done with the same site dataset (Montagnani et al., 2018; Zanotelli et al., 2019, 2015, 2013), we did not apply any u* filtering to exclude low turbulence conditions. Instead, we used the Foken and Wichura (1996) QA/QC approach for detecting and removing the data of poor quality. In our quality-controlled dataset, we kept the best quality data only, corresponding to classes 1–3 in the nine levels of the selected QA/QC classification. After the removal of low-quality flagged data, gap filling was performed according to Reichstein et al. (2005) using the online processing tool hosted at the Max Planck Institute for Biogeochemistry of Jena (http://www.bgc-jena.mpg.de/bgc-mdi/html/eddyproc/). The same tool was used to perform the partitioning of the measured NEE into GPP and ecosystem respiration (R_{eco}), adopting the method based on nighttime data (Reichstein et al., 2005). The raw measured ETa values were adjusted by forcing the closure of the energy budget according to the Bowen ratio method (Foken, 2008; Mauder et al., 2018; Twine et al., 2000) as described in Zanotelli et al. (2019).

Meteorological data were available from 2009 to 2018 thanks to the presence of a net radiometer (CNR1, Kipp and Zonen, Holland), a PAR quantum sensor (SKP 215, Skye Instruments Ltd., UK), and a thermohygrometer for air temperature and moisture data (HMP110, Vaisala, Finland), a professional rain-gauge for rainfall assessment (RAIN-O-MATIC, Pronamic, Silkeborg, Denmark). Meteorological data were taken at 0.1 Hz frequency and collected at 30 min intervals by a CR3000 data logger (Campbell Scientific, USA).

2.3. Identification of heat waves

To identify the presence of heat waves in the three summer months (June-August), the CTX90pct index described by Perkins and Alexander (2013) was used. The CTX90pct uses as threshold the calendar day 90th percentile of T_{max}, based on a 15-day window centered on the day. More in detail, we calculated for each summer day (June-Aug) the min and max values of T_{max} for the period 2009–2018, recorded at the experimental site, and, using a moving window of 15-days centered on each day, defined the 90th percentile of T_{max} for each summer day. Then, T_{max} values for each summer day in the 6-year period were compared with the 90th percentile threshold and whenever values were above the threshold for three consecutive days, a heat wave event was identified (Perkins, 2015).

We have characterized each year according to the heat waves using the following indexes: the yearly number of heat wave (HWN), the length of the longest yearly heat wave (HWD), the yearly sum of days participating in heat wave events (HWF), the average heat wave magnitude (HWM) and the hottest day (or peak) of the hottest yearly (HWA) (Perkins and Alexander, 2013). Each single heat wave has been further characterized by its duration, by its average T_{max} values, by the number of days preceding the heat wave with increasing T_{max}, by the daily temperature increase in the days preceding the heat wave and by the increase of T_{max} during the heat wave as compared to the week before (°C).

2.4. Response of ETa, NEE and GPP to T_{max}

Linear regression analysis between maximum daily air temperature versus ETa, NEE and GPP was performed using both the entire dataset and data from single years. Daily T_{max} data were binned in 1 °C temperature and average flux data (with their variability) were reported in temperature bins (Niu et al., 2012). As rain and overhead sprinkler irrigation decreased ETa and GPP and caused less negative or even positive NEE values, only days without rain and overhead irrigation events were considered in the analysis.

2.5. Energy partitioning during the heat waves

The available energy, equal to the difference between net radiation (Rn) and the soil heat flux (G), was calculated at a daily time scale and set equal to the sum of sensible (H) and latent (λE) after the closure of the energy balance carried out by attributing the residual energy to both H and λE according to the Bowen-ratio (H/ λE) (Twine et al., 2000; Wohlfahrt et al., 2009). The available energy (Rn-G), as well as its λE and H component during the 13 heat waves (total number of days = 57) and the Bowen-ratio, were compared with respect to the average of all summer days (including all the available data of June, July and August of the six years, n = 552), by means of a two sample Welch t-test. Moreover, by means of a one-sample t-test, we tested whether the percentual variation the four variables during the heat waves (n = 13) with respect to the average of the preceding week, was significantly different from zero.

2.6. Changes of NEE, GPP and ET during heat wave occurrence

After having checked the normal distribution of ETa, NEE and GPP data for each summer month, flux values occurring during the heat waves were converted into their normal deviate z values, which were tested against the entire population to identify z-score anomalies (Xu et al., 2020). A z-score higher than 1.65 or lower than − 1.65 denotes a flux value occurring with less than 10% probability, while values higher than + 1.98 or lower than − 1,98 denote fluxes occurring with less than 5% probability (Hoshmand, 1998).

For each heat wave event, we calculated the average ETa, NEE and GPP values during the heat wave and in the week before its occurrence. Rainy days and days when overhead irrigation was carried out were excluded from the average. One sample t-test was used to test the hypothesis that the % variation of the ETa, NEE and GPP fluxes occurring one week before the heat wave with respect to those occurring during each heat wave period (n = 13), were significant different from zero. The same procedure was carried out for relevant meteorological variables (T_{max}, PAR and VPD) and indexes (Bowen ratio and water use efficiency).

A multiple regression analysis was carried out to test the effect on the absolute and relative (as %) change of ETa, NEE and GPP during the heat wave period compared to the week before (dependent variables), due to either the characteristics of the period preceding the heat wave or of the heat wave itself. Regressors were:

a) number of days preceding the heat wave with increasing T_{max}
b) daily temperature increase in the period preceding the heat wave (°C)
c) average T_{max} during the week before the heat wave (°C)
d) length of the heat wave (days)
e) average T_{max} during the heat wave (°C)
f) increase of T_{max} during the heat wave compared to the week before (°C)

Before running the analysis, the presence of any autocorrelation among regressors was checked. As both regressor e) and f) were correlated with regressor c), we have run two separate analyses one with e) and f), but without c) (Model 1), and one with c), but without e) and f) (Model 2). Regressors a) and b) are a proxy of the gradualness of T increase in the period before the onset of the heat wave, intended as the slope of T_{max} increase before the heat wave begins (a graphical representation of this concept is given in fig. S3) Regressors d) and e) are proxy of the intensity of the heat wave. Regressor c) and f) have been added to test the hypothesis that the response to heat waves depends on the temperature before the heat wave and on the increase of the temperature before and during the heat wave. The week before has been chosen as a reference period to properly take into consideration the climatic conditions anticipating the heat wave event.

3. Results

3.1. Heat waves occurrence

The summer period considered in our study had a markedly different meteorological regime depending on the year, with 2014 and 2015 being the coldest and the warmest years, respectively (Fig. 1 and Table S1). July was, on average, the hottest summer month. The average T_{max} in June and August of 2017 and 2018 and in August 2013 was also markedly high (Table 1). Soil moisture data for the whole summer, including the periods when heat wave occurred (Fig. 2), mainly ranged between 0.30 and 0.35 $m^3 m^{-3}$; considering that the maximum soil water holding capacity for this soil is around 0.37 $m^3 m^{-3}$, this indicates no soil moisture limitations for tree uptake during the experimental period.

From 2009–2018, we identified 21 heat waves, while in the period when flux data were recorded (2013–18), the heat wave events were 14 (Fig. 2 and Table 2). One heat wave in August 2015 was not considered in the analysis as it started only 2 days after the end of a previous heat wave. The remaining 13 heat waves have been numbered in Table 2 according to the date they occurred and details for each heat wave are given. A schematic representation of the selected heat waves is reported in Fig. S3. The highest number of heat waves were recorded in 2015 (Fig. 2 and Tables 2 and 3). The two hottest days of the hottest yearly event (HWA) were recorded in 2015 and 2018 (Table 3) with T_{max} reaching almost 37 °C. Five of the 14 heat waves according to CXT90pct index occurred in June, 3 in July and 6 in August. Heat waves differed as to their duration (from 3 to 8 days) and average T_{max} (31.8–35.4) (Table 2). The period immediately before the heat wave was quite variable in terms of daily T_{max} increase: some heat waves were anticipated by a rapid temperature increase, while for other heat waves, the temperature was already relatively high in the period before the heat wave (Fig. 1 and Table 2). The gradualness of temperature increase before the onset of the heat wave differed from 2.75 °C per day, on average, for three consecutive days (HW2), to 0.56 °C per day, on

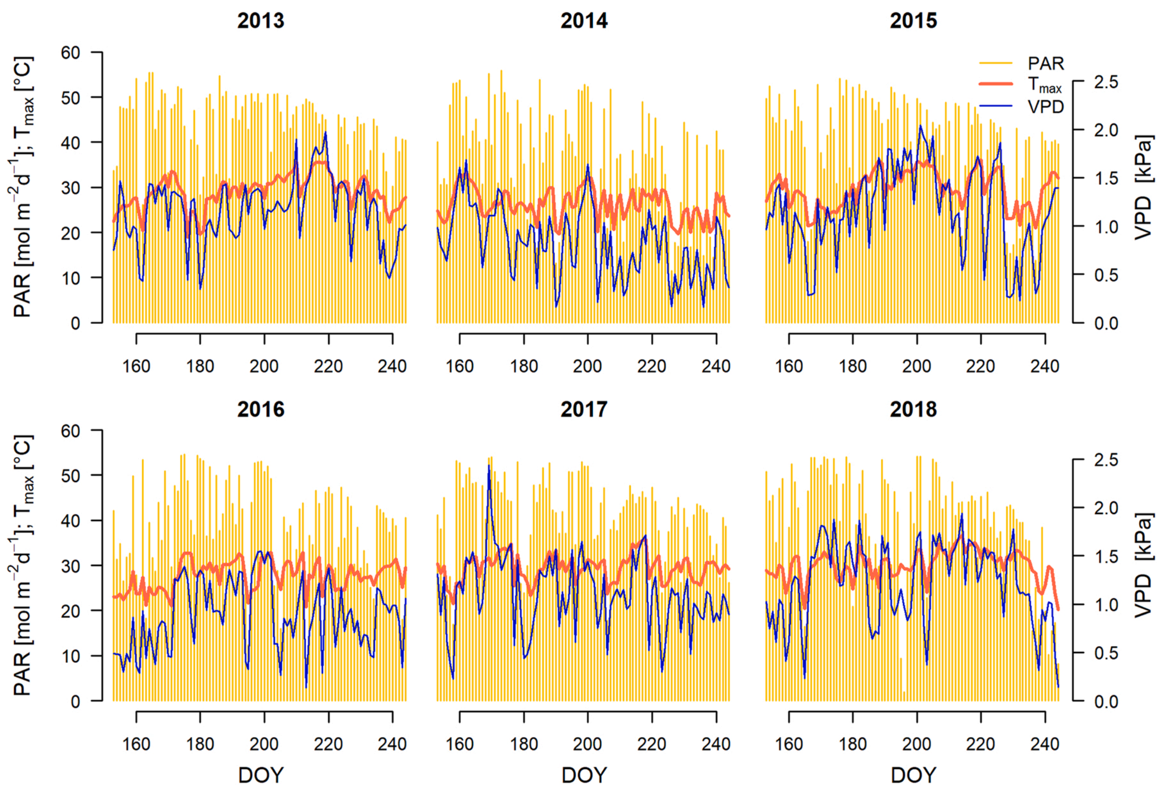

Fig. 1. Meteorological trend during the three summer months of the six-year period in which the occurrence of heat waves was analysed. Each plot reports the pattern of the maximum daily temperature (T_{max}, °C), the photosynthetic active radiation (PAR, *mol m*$^{-2}$ *day*$^{-1}$), and the vapor pressure deficit (VPD, kPa) from DOY 153 (begin of June) to DOY 244 (end of August).

Table 1
Monthly cumulated rainfall (mm) and averages of minimum (T_{min}) and maximum (T_{max}) summer temperatures (°C) during the months of heat wave occurrence and for the years considered in this study.

year	Rainfall (mm)			T_{min}			T_{max}		
	Jun	*Jul*	*Aug*	*Jun*	*Jul*	*Aug*	*Jun*	*Jul*	*Aug*
2013	89.0	68.6	87.4	13.4	16.8	16.2	26.6	30.3	29.8
2014	95.8	149.6	115.0	13.9	15.6	14.9	27.0	26.5	25.1
2015	59.6	27.8	98.6	14.7	18.8	16.7	27.2	32.4	29.1
2016	100.6	79.7	67.8	14.4	16.8	15.1	26.1	28.9	27.9
2017	100.3	109.8	120.6	16.1	15.9	15.7	29.1	29.4	29.8
2018	51.5	91.4	94.8	14.8	16.7	16.9	29.0	30.6	30.7
2013–18	*82.8*	*87.8*	*97.4*	*14.6*	*16.8*	*15.9*	*27.5*	*29.7*	*28.7*

average, for 4 consecutive days (see Fig. S3 for a graphical representation of the heat waves).

3.2. The response of ETa, NEE and GPP to T_{max}

Considering the entire period, in spite of the variability of ETa values within 1 °C bin, there was a linear increase of ETa at increasing daily T_{max} (Fig. 3a). Most summer ETa data ranged between 4 and 6 mm day^{-1}. The variability of ETa values within each 1 °C bin (Fig. 3a) was especially high in the range 25–31 °C. The linear regression between ETc (dependent variable) and T_{max} (independent variable) was significant in all years, except 2016, with similar slopes in all the years (0.163–0.169 mm ETa day^{-1} °C^{-1}), but in 2014 (Fig. 4a and Table 4). Summer 2014 and 2016 were the two coldest in the considered period.

Differently from ETa, NEE and GPP were not linearly related to T_{max} when the six-year data were considered together (Fig. 3b and c). The variability of NEE and GPP values within each 1 °C of T_{max} bin was in fact rather high and both average NEE and average GPP were similar across the entire temperature range. Significant linear regression between T_{max} vs. NEE (positive) and T_{max} vs. GPP (negative) were however recorded in 2013 and 2015, with similar slopes in years (NEE= 0.21–0.22 g C m^{-2} day^{-1} °C^{-1}; GPP= −0.16 to −0.19 g C m^{-2} day^{-1} °C^{-1}) (Fig. 4b and c, and Table 4).

3.3. Effects of the heat waves on energy partitioning

The available energy (Rn-G) significantly increased (p-value < 0.001) by 16% during the heat waves (Fig. 5), passing from an average value of 13.6 MJ m^{-2} day^{-1} during the summer season (June-August, 552 data available) to the average of 15.8 MJ m^{-2} day^{-1} during an heat wave event (57 days selected). The partitioning between λE and H also changed (Fig. 5), with a significant increase (p-value <0.001) of λE (+ 22%, from 12.4 to 15.1 MJ m^{-2} day^{-1}) and a reduction (p-value <0.01) of H (−37%, from 1.2 to 0.8 MJ m^{-2} day^{-1}). Accordingly, a significant reduction by 52% (p-value <0.001) of the Bowen-ratio was observed when confronting the average value during the entire summer and during the heat wave. The change of the partitioning of the available energy during the heat waves was confirmed by the increase of the λE (+

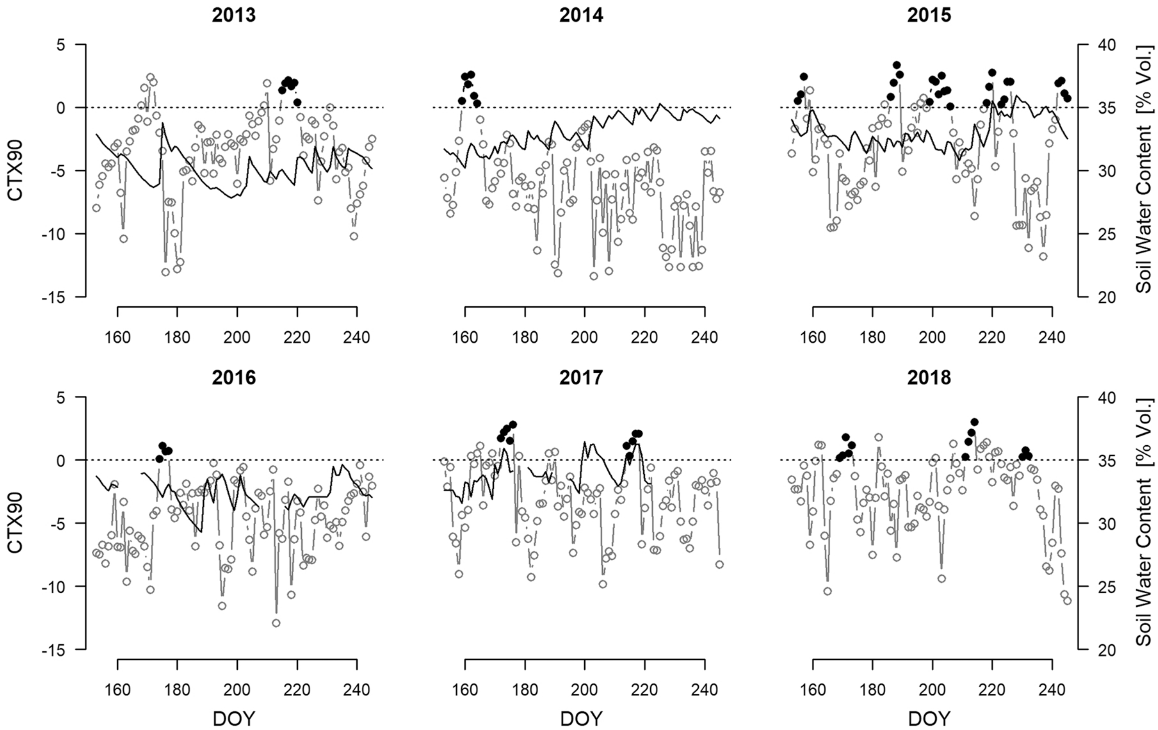

Fig. 2. Pattern of CTX90pct index (empty dots) and volumetric soil moisture (straight line) across the summer period of 2013–18. Heat waves were selected whenever CTX90pct index was > 1 for three consecutive days and depicted by solid dots.

Table 2
Main characteristics of each heat wave and of the preceding period (7 days).

HW number	Beginning of the HW (day/month/year)	HW length (days)	Average of T_{max} values in the week before the HW (^oC)	Average of T_{max} values during the HW (^oC)	Days preceding the HW with continuous T_{max} increase	Average T_{max} increase in the period before the HW (^oC day^{-1})
1	2/8/13	5	32.77	35.38	3	1.51
2	7/6/14	6	25.36	32.17	3	2.75
3	3/6/15	3	27.74	31.81	3	2.43
4	4/7/15	4	30.77	34.68	4	0.56
5	17/7/15	8	32.28	34.63	4	0.67
6	5/8/15	3	31.46	35.33	5	1.30
7	29/8/15	4	29.41	32.45	3	1.28
8	23/6/16	3	27.06	32.72	5	2.03
9	20/6/17	5	31.01	33.65	2	1.50
10	1/8/17	5	28.40	35.01	5	1.79
11	17/6/18	5	30.30	32.01	3	1.19
12	29/8/18	4	32.05	35.38	1	2.61
13	17/8/18	3	31.53	32.89	1	1.67

Table 3
Heat waves yearly occurrence and characteristics according to the CTX90pct index.

HWs description indexes	2009	2010	2011	2012	2013	2014	2015	2016	2017	2018
HWN (yearly number of heat waves)	1	2	1	3	1	1	6	1	2	3
HWD (length of the longest yearly event, days)	4	4	7	6	5	6	8	3	5	5
HWF (yearly sum of participating heat wave days)	4	7	7	14	5	6	26	3	10	13
HWM (average magnitude of all yearly heat waves,^oC higher than the 90th percentile)	1.19	1.26	1.59	2.35	1.80	1.43	1.50	0.84	1.78	0.96
HWA (hottest day of hottest yearly event, $T_{max}$$^oC$)	33.92	35.60	34.50	35.43	35.64	33.31	36.00	32.82	35.74	36.77

5%, p-value <0.05) and the decrease of the Bowen ratio (−46%, p-value <0.05) with respect the week preceding each heat event, while the available energy was not statistically different (Table 5).

3.4. Effects of heat waves on ETa, NEE and GPP

ETa values during all heat waves were always higher than the average ETa values for the month they occurred (z-scores >0, Fig. 6). The magnitude of the effects varied with the heat wave. When the original flux data during the heat wave were converted into z-scores, we could assess how anomalous the flux was with respect to the period it occurred. Heat waves 1, 6, 8, 9, 10, 11 had a z-score > 1.98 (Fig. 6) corresponding to a probability lower than 5%, while heat waves 2, 4 and 5 had z-scores >1.68, corresponding to a probability lower to 10% to

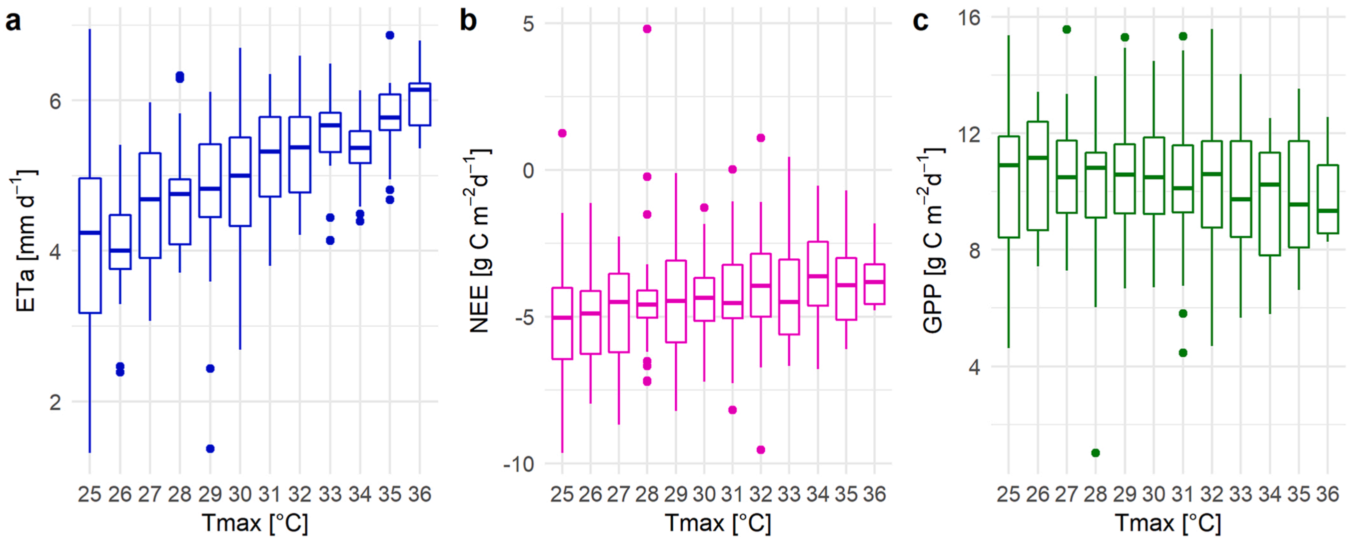

Fig. 3. ETa (a), NEE (b) and GPP (c) measured across the summer of the 2013–18 period and averaged for 1 °C of T_{max} bins. Boxes include 50% of the data. Bars indicate the upper and lower quartile; dots are the outliers, i.e., all data that falls above (or below) 1.5 the interquartile range plus the third (or minus the first) quartile, respectively. Only days without rainfall and without irrigation are included in the figure.

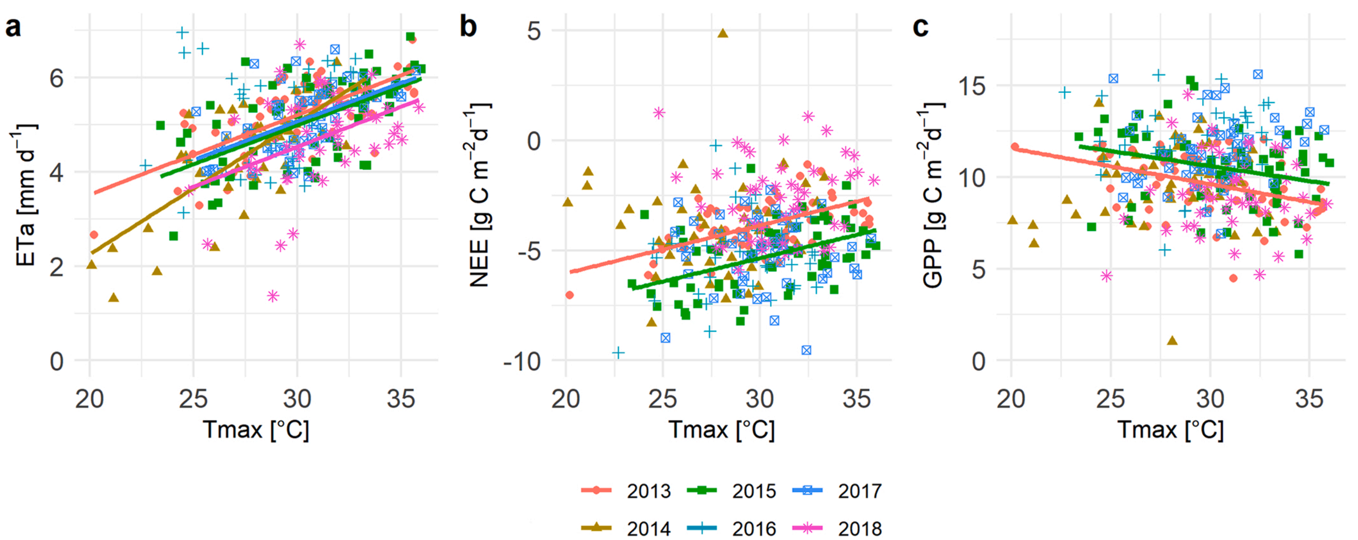

Fig. 4. ETa (a), NEE (b) and GPP (c) daily values of the summer months (2013–2018) plotted against concurrent daily T_{max} data. Each year is represented by different colours. Lines indicate significant linear regression between the two variables, and the respective parameters are reported in Table 4.

randomly occur. Differently from ETa, z-score values for NEE were sometimes positive and sometimes negative, but never indicated the presence of anomalies. The GPP fluxes during eight heat wave events corresponded to z-score values close to zero, indicating that GPP values during the heat waves are among those occurring with high frequency. Interestingly, when the z-score was positive for NEE, the GPP showed a negative z-score, often of the same magnitude, and vice versa (Fig. 6).

Considering all the heat wave events together, ETa was on average 8% higher (+ 0.37 mm day^{-1}) during the heat wave period compared to the week before its occurrence (Table 5). As indicated by the results of the multiple linear regression analysis (Table 6), ETa increase was not always the same, but depended mainly on the T_{max} difference during the heat wave and in the week before (model 1, positive relationship), and on the average T_{max} in the week before the heat wave (model 2, negative relationship). Such effects are also visible in Fig. 7a. To a less extent, also the duration of the heat wave (positive relationship in both models, Table 6) affected the ETa increase during the heat wave. The onset gradualness of the heat wave (regressors a and b) had, on the contrary, no effect on the ETa increase (Table 6).

Neither NEE nor GPP was affected by the onset of the heat wave when all the events were considered together (Table 5). None of the examined characteristics, neither in the period preceding the heat wave nor during the heat wave itself affected the response of NEE to heat wave (Table 6). The change of GPP during the heat wave as compared to the week before was, however, affected by the average T_{max} during the heat wave (model 1, positive relationship) and by the T_{max} in the week before the heat wave (model 2, positive relationship). According to both models, the number of consecutive days with increasing T_{max} before the heat wave additionally affected the change of GPP during the heat wave as compared to the week before (both models, negative relationship) (Table 6). In addition to λE and Bowen ratio, a significant variation during the heat wave with respect to the week before was observed in the T_{max} (+ 11%, + 3.31 °C), in the VPD (+ 23%, + 0.25 kPa), while the PAR and water use efficiency did not significant change (Table 5).

Table 4
Coefficients of determination (R^2), significance and slope of the linear regression between daily water and C fluxes (ETa, mm H_2O m^{-2} day^{-1}; NEE and GPP, g C m^{-2} day^{-1}) and daily T_{max} (°C) for the summer period of each single year and for the entire period. A graphical representation of the correlation is reported in Fig. 4.

Flux	2013	2014	2015	2016	2017	2018	2013–18
ETa *(mm H_2O day^{-1} °C^{-1})*							
R^2	0.48	0.60	0.36	0.05	0.34	0.17	0.31
Sign.	***[a]	***	***	n.s.	***	**	***
Slope	0.168	0.279	0.165	0.082	0.163	0.170	0.170
NEE *(g C m^{-2} day^{-1} °C^{-1})*							
R^2	0.34	0.00	0.22	0.03	0.00	0.00	0.04
Sign.	***	n.s.	***	n.s.	n.s.	n.s.	n.s.
Slope	0.217	0.008	0.212	0.121	-0.004	0.032	0.119
GPP *(g C m^{-2} day^{-1} °C^{-1})*							
R^2	0.15	0.01	0.07	0.01	0.05	0.00	0.005
Sign.	**	n.s.	*	n.s.	n.s.	n.s.	n.s.
Slope	-0.195	0.081	-0.164	0.061	0.164	-0.016	-0.051

[a] *, **, *** and n.s. = significant with $P \leq 0.05$, 0.01, 0.001 and not significant, respectively.

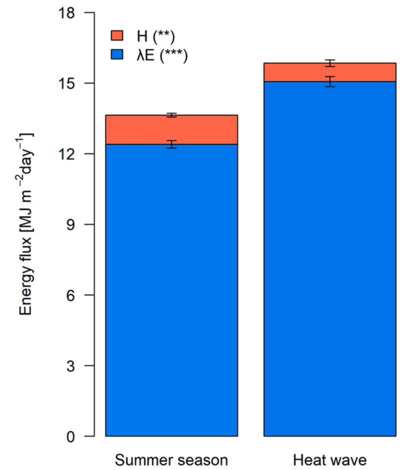

Fig. 5. Average daily available energy (Rn-G, MJ m^{-2} day^{-1}) during the summer months (June – August of six years, n = 552 days) and during the heat waves events (n = 57 days), partitioned into the two components of latent (λE) and sensible heat (H). The asterisks indicate a significant difference of each component between the two selected periods (*** = p-value <0.001; ** = p-value <0.01).

4. Discussion

With a global cultivation area of approximately 5 million ha (1 of which in Europe) and a fruit production ranging from 80 and 90 million of tons $year^{-1}$ (FAOSTAT, 2021), apple represents one of the most relevant fruit tree crop worldwide. The predicted climate scenarios, which foresee an increase in temperature peaks and frequency of extreme heat and drought events (IPCC, 2018), pose a threat to the apple industry. There is extensive literature about the effects of high summer temperature on fruit damages by sunburn (Felicetti and Schrader, 2008; Kalcsits et al., 2017; Olivares-Soto et al., 2020; Schrader, 2011; Yuri et al., 2019, 2010), but less is known about the eco-physiological response of the apple orchard during the heat waves. The effects of heat waves on CO_2 and H_2O fluxes have been assessed in several terrestrial ecosystems, where high temperatures have been usually accompanied by drought stress (Rita et al., 2020; Ruehr et al., 2015; Stéfanon et al., 2014; Von Buttlar et al., 2018). By contrast, in the present study, the heat wave events occurred when soil moisture was adequate to support tree water uptake. Such a fundamental difference must be born in mind in order to explain the main results we obtained.

Reichstein et al. (2013) highlighted the main characteristics in which croplands differ from other ecosystems with respect to carbon-cycle responses to climate extremes. These includes a) the management interventions (such as irrigation) that can trigger changes on short timescales, b) the fact that agro-ecosystems are reset annually (either completely or partially in annual and perennial crops, respectively) with a fraction of vegetated land cover that substantially changes during the season, and c) the nature and extent of human interventions on each specific crop, that makes the prediction of the response to extremes of these systems highly uncertain and crop-specific (Deb Burman et al., 2020; Reichstein et al., 2013).

The definition of heat wave has been a matter of discussion among the scientific community (Perkins and Alexander, 2013). In our study, the heat wave refers to at least 3 consecutive days of unusually high maximum temperature for the period of the year they occur. One major consequence of such an approach is that the heat waves were characterized by differences in maximum temperatures depending on the summer period they occurred. The most severe heat wave in terms of T_{max} and length were those occurring between July and the first decade of August (with averages T_{max} close to 35 °C). Summer storms, frequent in the experimental area surrounded by mountains, normally interrupted the heat wave (see also Fig. 1), whose duration varied from 3 to 8 days (Table 2).

To allow a better comparison of our data with literature, it is worth underlining that T_{max} values were measured at 8 m height and such data are highly correlated (R^2 =0.97) with T_{max} at 2 m measured in a close weather station located in the middle of a grassed area. The maximum peaks recorded during the heat wave would have been approx. 0.5 °C higher if measured at 2 m height. The highest T_{max} recorded this study approached 37 °C, a value markedly lower than those reported in other agricultural areas where the effects of excessive summer temperatures well above 40 °C, have been studied (Olivares-Soto et al., 2020; Wand et al., 2008; Yuri et al., 2010).

During heat waves, the λE fraction increased both in relation to the average day of the entire summer (Fig. 5) and when compared with the week before the heat waves (Table 5). This evidence indicates that in the studied apple orchard, contrary to what happens in un-managed ecosystems (Teuling et al., 2010), approx. 95% of the available energy during an heat wave is dissipated as latent heat (Table 5). This evidence supports the hypothesis of a significant transpiration cooling effects of irrigated apple leaves found elsewhere (Solomakhin and Blanke, 2010). If and to which extent the large areas devoted to irrigated apples may exert a direct mitigation role on local temperatures extremes deserves further investigation (Langworthy et al., 2020; Thiery et al., 2020, 2017).

In nine of the 13 heat waves, ETa was exceptionally high, with values laying within summer records occurring with less than 10% frequency, and during 6 of them the ETa was among the 5% highest summer values (Fig. 6). Daily ETa values in summer were positively related to daily T_{max} across the entire range, from 26 to 36 °C. Elevated air temperatures in summer affect VPD, which together with PAR represent the main driver of ET in the apple orchard (Montagnani et al., 2018). With the exception of the 2014 and 2016, when summer was mild and wet, the T_{max}-dependent ETa increase calculated across the entire T_{max} range was similar in all years and ranged from 0.163 to 0.169 mm day^{-1} °C^{-1}. A closer look at the ETa response to T_{max} during the events of extremely high temperature suggests, however, that ETa response to T_{max} increases is less pronounced, although still significant, in the upper range of T_{max} values. A first evidence in this respect appears by comparing the 0.112 mm day^{-1} °C^{-1} ETa increase during the heat wave as compared to the week before (calculated from Table 5), algebraically lower that the values recorded across the entire T_{max} range (see “slope” in Table 4). Additionally, the results of the multiple regression analysis (model 2) showed that the ETa increase during the heat wave was progressively less intense when the onset of the heat wave was preceded by a warm week (see parameter “c” in model 2, Table 6).

The general increasing ET trend occurring during the heat waves we

Table 5
Average values of ETa (mm H_2O day^{-1}), NEE; GPP (g C m^{-2} day^{-1}), the main environmental variables: T_{max} (°C), PAR (mol m^{-2} day^{-1}) and VPD (kPa), the Bowen ratio (unitless) and the water use efficiency (WUE, g C kg H_2O^{-1}) in the week preceding the heat wave (HW) and during the heat wave itself. A t-student test was applied to test whether the average relative (%) change of each variable during heat wave with respect to the preceding period was significant (*** = p-value <0.001; ** p-value < 0.01; * p-value < 0.05, n.s not significant).

Variable	Average of the week before HW (± s.e.)	Average of the HW period (± s.e.)	% variation (± s.e. and t.test)
ETa (*mm day^{-1}*)	5.07 ± 0.20	5.44 ± 0.19	+ 8.06 ± 3.20 *
NEE (*g C m^{-2} day^{-1}*)	-3.90 ± 0.53	-3.57 ± 0.48	+ 11.42 ± 19.66 $^{n.s}$
GPP (*g C m^{-2} day^{-1}*)	9.77 ± 0.59	9.56 ± 0.51	-0.69 ± 3.74 $^{n.s}$
T_{max} (*°C*)	30.39 ± 0.66	33.70 ± 0.39	+ 11.30 ± 1.80 * **
PAR (mol m^{-2} day^{-1})	45.22 ± 1.02	45.56 ± 0.92	+ 1.00 ± 1.47 $^{n.s}$
VPD (kPa)	1.23 ± 0.07	1.48 ± 0.06	+ 22.59 ± 5.23 * **
WUE (*g C kg H_2O^{-1}*)	1.95 ± 0.12	1.78 ± 0.10	-6.52 ± 5.3 $^{n.s.}$
Rn - G (MJ m^{-2} day^{-1})	15.57 ± 0.39	15.86 ± 0.38	+ 2.23 ± 2.35 $^{n.s.}$
λE (MJ m^{-2} day^{-1})	14.21 ± 0.37	14.91 ± 0.38	+ 5.31 ± 2.62 *
H (MJ m^{-2} day^{-1})	2.29 ± 0.85	0.96 ± 0.22	-41.54 ± 26.25 $^{n.s.}$
Bowen-ratio	0.11 ± 0.02	0.07 ± 0.02	-45.57 ± 23.90 *

observed contrasts with previous studies carried out in grasslands and forest sites (Li et al., 2021; Seneviratne et al., 2010) that, with few exceptions (Lindroth et al., 2020) have recorded a reduction of ET during excessive heat periods, a fact that has been explained considering that hot summers in rain fed agricultural systems and in forests, are often accompanied by drought. The methodology we employed to quantify water fluxes does not distinguish between evaporation and transpiration. However, having excluded from our analysis all summer rainy days, we can speculate that apple trees under optimal water supply keep stomata open during high summer temperatures, an effective cooling mechanism that develops at the leaf level, which produces tangible results in mitigating heat waves effects even at a regional scale (Langworthy et al., 2020; Li et al., 2020; Solomakhin and Blanke, 2010; Thiery et al., 2020). Further investigations, using experimental approaches that uncouple evaporation from transpiration, are necessary to verify this hypothesis. The response of NEE and GPP to heat waves is more complex than that recorded for ETa. NEE (= -NEP, Net Ecosystem Productivity) represents the net CO_2 flux from the soil-vegetation to the atmosphere. Negative values indicate net photosynthesis (Pn) higher than ecosystem respiration (Re). Any change of Pn and Re could affect NEE fluxes and even results in no change of NEE if they both respond in the same way, offsetting each other.

Both NEE and GPP fluxes occurring during the heat waves events laid well within the most frequent flux values recorded in summer (Fig. 6) and in none of the flux was considered an extreme score. In addition, neither NEE nor GPP changed during the heat wave events as compared to the week before (Table 5). Taken together, these results suggest that both fluxes are rather unaffected by the heat waves and that other factors are responsible for the variability of the daily C fluxes in summer. If our data show no clear short term response of GPP and NEE to the onset of the heat wave, they, however, do not rule out the influence of the maximum daily temperature in summer on NEE and GPP. In the two hottest years (2013 and 2015), in fact, in spite of the rather low R^2 values, which suggest the presence of additional drivers, NEE increased and GPP decreased moving from low to high daily T_{max} values. Interestingly, the increasing rate of NEE to increasing T_{max} was rather constant in the two years (on average 0.215 g C m^{-2} day^{-1} °C^{-1}) and slightly higher, in absolute value, than the decrease of GPP (on average 0.175 g C m^{-2} day^{-1} °C^{-1}). Data suggest that the decrease of GPP to T_{max} in the summer 2013 and 2015 accounted for most of the NEE increase. The response of NEE to air temperature, if measured across a wide temperature range tends to follow a peak curve, as shown by Niu et al. (2012) across a large number of terrestrial ecosystems: at increasing temperatures, NEE decreases (higher absolute values) until an optimum temperature is reached and then it increases, causing a loss of the ecosystem ability to act as a C sink. Moreover, ecosystem respiration has been demonstrated to be directly related to the rate of GPP in both its autotrophic and heterotrophic component (Amthor, 2000; Reich et al., 2006; Scandellari et al., 2015). In a recent cross-ecosystem analysis, Xu et al. (2020) have found that GPP tends to decrease as a response to heat waves in all tree ecosystems, and that such effect lasts several days after the heat wave ceased. Although we could not assess a general pattern of GPP response to all heat waves (Table 5), the multiple regression models highlighted a significant effect of two parameters: the number of days with continuous temperature increase, and the T_{max} during the heat wave or in the preceding week, that could help to predict the expected change in GPP. It tended to decrease (heat waves 2, 3, 8 and 11) when the T_{max} in the preceding period was low, while it was irresponsive to or even increased during the most extreme heat wave (HWs 1, 5, 9, 12 and 13) that were preceded by a week of relatively high T_{max} (Table 6), possibly as a result of tree acclimation (Greer, 2015b).

Given the ecosystem-scale nature of the eddy covariance measurements, it has to be considered that ET, NEE and GPP fluxes also average the contribution of the herbaceous vegetation present in the orchard alleys, which might increase or decrease its GPP during the heat wave, if C_4 or C_3 species are present, respectively (Xu et al., 2020). In the same orchard used in this study, Zanotelli et al. (2013) estimated that the

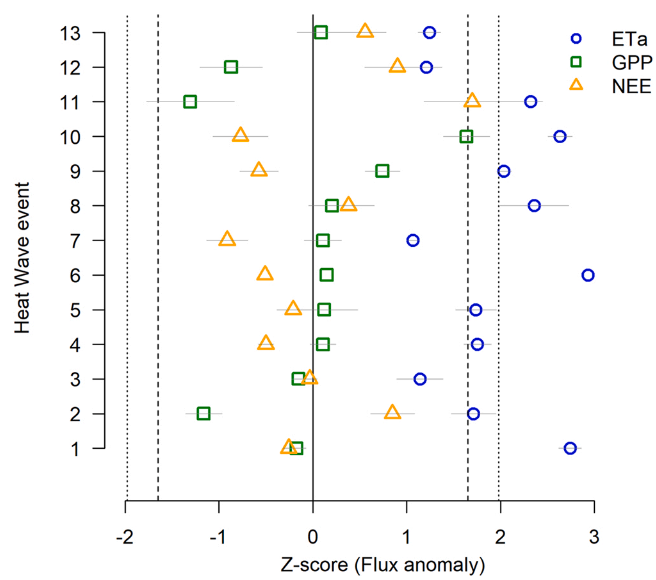

Fig. 6. Averaged daily ETa (circles), NEE (triangles) and GPP (squares) anomaly (z-score) during the 13 heat waves listed in Table 2. The error bars stand for standard errors. The vertical dashed and dotted lines indicate the z scores of 1.68 and 1.98, which correspond to events occurring with 10% and 5% probability, respectively.

Table 6
Multiple regression models relating the differences of ETa (mm H_2O day^{-1}), NEE and GPP (g C m^{-2} day^{-1}) fluxes between the heat wave period and the preceding 7-days to either the characteristic of the period preceding the heat wave or of the heat wave itself. The coefficient of determination (R^2), the p-value and the Akaike information criterion (AIC) are reported for each model together with the relative importance of the parameters included the models.

Dependent variable (y)	Minimum adequate model (MAM)	R^2	*p-value*	AIC	relative importance of the parameters (sum = 1)
ΔETa	*Model 1* $y = 3.3358 + 0.0941d - 0.1217e + 0.2158f$	0.6530	0.01862	15.23	*d*= 0.086; *e*= 0.148; *f*= 0.765
(mm day⁻¹)	*Model 2* $y = 5.3694 - 0.1785c + 0.0983d$	0.6159	0.00836	14.56	*c*= 0.901; *d*= 0.099
ΔNEE	*Model 1* $y = 16.9406 - 0.4933e$	0.2689	0.06942	45.39	*e* = 1.000
(g C m⁻² day⁻¹)	*Model 2* $y = 7.7142 - 0.2465c$	0.1733	0.15710	46.99	*c*= 1.000
ΔGPP	*Model 1* $y = -16.905 - 0.5255a + 0.5452e$	0.6658	0.00417	33.58 38.19	*a*= 0.459; *e*= 0.541
(g C m⁻² day⁻¹)	*Model 2* $y = -7.8879 - 0.2791a + 0.2853c$	0.5238	0.02448		*a*= 0.327; *c*= 0.673

Explicative notes for Table 6:
List of parameters considered in MRM Parameter description
a number of days preceding the HW with increasing T_{max}
b daily temperature increase in the period preceding the HW (°C)
c average T_{max} during the week before the HW (°C)
d length of the HW (days)
e average T_{max} during the HW (°C)
f increase of T_{max} during the HW compared to the week before (°C)

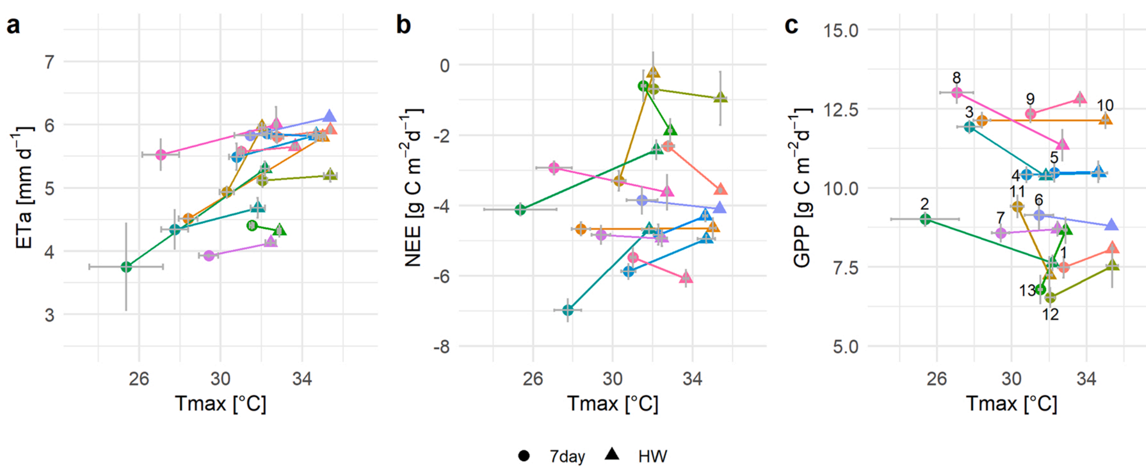

Fig. 7. Average ETa (a), NEE (b) and GPP (c) plotted against the average T_{max} occurring in the week before each heat wave (pre-HW, dots) and during each heat wave (triangles). Bars represents standard error for both flux and T_{max} during each heat wave event. The colours refer to each single heat wave event, as identified with numbers in plot *c* and listed in Table 2.

herbaceous vegetation in the alleys accounts for approximately 5% of total net primary production of the whole orchard, with most species showing a C3 photosynthetic pathway.

5. Conclusions

This case study has offered the possibility to assess the response of energy, carbon, and water fluxes at the ecosystem scale of a well-watered apple orchard during unusually high summer temperatures. The fraction of available energy dissipated by the ecosystem as λE increased significantly during the heat wave events, causing a decrease of the Bowen-ratio. During 9 out of the 13 heat waves, ETa records were among the 10% highest values ever recorded in summer. ETa increased at increasing T_{max} values over a rather wide range of temperatures (from 25° to 35°C), but the increase was less pronounced, although still significant, in the upper range of T_{max} values, that typically occur during heat waves. Conversely, the response of C fluxes to the highest temperatures was not so univocal, with a slight, but significant reduction of C assimilation with respect to T_{max} observed only in the 2 hottest years. Carbon flux anomalies were either positive or negative depending on the heat wave event. The contrasting pattern of ET and GPP observed during the heat waves suggests a reduction of the water use efficiency of the orchard during anomalously hot summer periods that could be exacerbated if summer T_{max} will increase further.

CRediT authorship contribution statement

Damiano Zanotelli: Investigation, Writing – original draft, Data curation, Methodology, Writing – review & editing, Visualization. **Leonardo Montagnani**: Investigation, Writing – review & editing, Supervision. **Carlo Andreotti**: Writing – review & editing, Resources, Formal analysis. **Massimo Tagliavini**: Conceptualization, Writing – review & editing, Supervision, Project administration, Software, Funding acquisition.

Declaration of Competing Interest

The authors declare the following financial interests/personal relationships which may be considered as potential competing interests: Massimo Tagliavini reports financial support was provided by Assomela Soc. Coop.

Acknowledgements

This work was financially supported by the following research projects: i) Water use efficiency across land use types in South Tyrol (acronym WEST, grant n. TN2059, financed by the Free University of Bolzano-Bozen, Italy); ii) Monitoring key environmental parameters in the alpine environment involving science, technology and application (acronym MONALISA, financed by the Autonomous Province of Bolzano-Bozen, Italy); and iii) Quality indicators and sustainable irrigation in apple production (acronym IQUIS, financed by Assomela Soc. Coop., Italy). The authors wish to thank Dr. Martin Thalheimer of the Laimburg Research Centre (BZ, Italy) for providing ancillary meteorological data, and the Department of Innovation, Research University and Museums of the Autonomous Province of Bozen/Bolzano for covering the Open Access publication costs.

Appendix A. Supporting information

Supplementary data associated with this article can be found in the online version at doi:10.1016/j.eja.2022.126460.

References

Allen, R.G., Walter, I.A., Elliott, R., Howell, T., Itenfisu, D., Jensen, M., 2005. The ASCE Standardized Reference Evapotranspiration Equation.

Amthor, J.S., 2000. The McCree-de Wit-Penning de Vries-Thornley respiration paradigms: 30 Years later. Ann. Bot. 86, 1–20. https://doi.org/10.1006/anbo.2000.1175.

Bastos, A., Gouveia, C.M., Trigo, R.M., Running, S.W., 2014. Analysing the spatio-temporal impacts of the 2003 and 2010 extreme heatwaves on plant productivity in Europe. Biogeosciences 11, 3421–3435. https://doi.org/10.5194/bg-11-3421-2014.

Chapin, F.S., Woodwell, G.M., Randerson, J.T., Rastetter, E.B., Lovett, G.M., Baldocchi, D.D., Clark, D.A., Harmon, M.E., Schimel, D.S., Valentini, R., Wirth, C., Aber, J.D., Cole, J.J., Goulden, M.L., Harden, J.W., Heimann, M., Howarth, R.W., Matson, P.A., McGuire, A.D., Melillo, J.M., Mooney, H.A., Neff, J.C., Houghton, R.A., Pace, M.L., Ryan, M.G., Running, S.W., Sala, O.E., Schlesinger, W.H., Schulze, E.D., 2006. Reconciling carbon-cycle concepts, terminology, and methods. Ecosystems 9, 1041–1050. https://doi.org/10.1007/s10021-005-0105-7.

Ciais, P., Reichstein, M., Viovy, N., Granier, A., Ogée, J., Allard, V., Aubinet, M., Buchmann, N., Bernhofer, C., Carrara, A., Chevallier, F., De Noblet, N., Friend, A.D., Friedlingstein, P., Grünwald, T., Heinesch, B., Keronen, P., Knohl, A., Krinner, G., Loustau, D., Manca, G., Matteucci, G., Miglietta, F., Ourcival, J.M., Papale, D., Pilegaard, K., Rambal, S., Seufert, G., Soussana, J.F., Sanz, M.J., Schulze, E.D., Vesala, T., Valentini, R., 2005. Europe-wide reduction in primary productivity caused by the heat and drought in 2003. Nature 437, 529–533. https://doi.org/10.1038/nature03972.

De Kauwe, M.G., Medlyn, B.E., Pitman, A.J., Drake, J.E., Ukkola, A., Griebel, A., Pendall, E., Prober, S., Roderick, M., 2019. Examining the evidence for decoupling between photosynthesis and transpiration during heat extremes. Biogeosciences 16, 903–916. https://doi.org/10.5194/bg-16-903-2019.

Deb Burman, P.K., Shurpali, N.J., Chowdhuri, S., Karipot, A., Chakraborty, S., Lind, S.E., Martikainen, P.J., Chellappan, S., Arola, A., Tiwari, Y.K., Murugavel, P., Gurnule, D., Todekar, K., Prabha, T.V., 2020. Eddy covariance measurements of CO_2 exchange from agro-ecosystems located in subtropical (India) and boreal (Finland) climatic conditions. J. Earth Syst. Sci. 129, 43. https://doi.org/10.1007/s12040-019-1305-4.

FAOSTAT, 2021. Food and agriculture data. http://www.fao.org/faostat/en/#data/QC. Data refers to years 2015–2019. Last access January 2021.

Felicetti, D.A., Schrader, L.E., 2008. Changes in pigment concentrations associated with the degree of sunburn browning of "Fuji" apple. J. Am. Soc. Hortic. Sci. 133, 27–34. https://doi.org/10.21273/jashs.133.1.27.

Foken, T., 2008. The energy balance closure problem: an overview. Ecol. Appl. 18, 1351–1367. https://doi.org/10.1890/06-0922.1.

Foken, T., Wichura, B., 1996. Tools for quality assessment of surface-based flux measurements. Agric. For. Meteorol. 78, 83–105. https://doi.org/10.1016/0168-1923(95)02248-1.

Frank, Dorothea, Reichstein, M., Bahn, M., Thonicke, K., Frank, David, Mahecha, M.D., Smith, P., van der Velde, M., Vicca, S., Babst, F., Beer, C., Buchmann, N., Canadell, J. G., Ciais, P., Cramer, W., Ibrom, A., Miglietta, F., Poulter, B., Rammig, A., Seneviratne, S.I., Walz, A., Wattenbach, M., Zavala, F.M.A., Zscheischler, J., 2015. Effects of climate extremes on the terrestrial carbon cycle: Concepts, processes and potential future impacts. Glob. Chang. Biol. 21, 2861–2880. https://doi.org/10.1111/gcb.12916.

Greer, D.H., 2015a. Seasonal changes in the photosynthetic response to CO_2 and temperature in apple (Malus domestica cv. 'Red Gala') leaves during a growing season with a high temperature event. Funct. Plant Biol. 42, 309–324. https://doi.org/10.1071/FP14208.

Greer, D.H., 2015b. Temperature-dependent responses of the photosynthetic and chlorophyll fluorescence attributes of apple (Malus domestica) leaves during a sustained high temperature event. Plant Physiol. Biochem. 97, 139–146. https://doi.org/10.1016/j.plaphy.2015.10.002.

Hoshmand, R.A., 1998. Statistical Methods for Environmental and Agricultural Sciences - 2nd. CRC Press.

IPCC, 2018. Summary for Policymakers. In: Global warming of 1.5°C. An IPCC Special Report on the impacts of global warming of 1.5°C above pre-industrial levels and related global greenhouse gas emission pathways, in the context of strengthening the global response to. https://doi.org/10.1017/CBO9781107415324.

Kalcsits, L., Musacchi, S., Layne, D.R., Schmidt, T., Mupambi, G., Serra, S., Mendoza, M., Asteggiano, L., Jarolmasjed, S., Sankaran, S., Khot, L.R., Espinoza, C.Z., 2017. Above and below-ground environmental changes associated with the use of photoselective protective netting to reduce sunburn in apple. Agric. For. Meteorol. 237–238, 9–17. https://doi.org/10.1016/j.agrformet.2017.01.016.

Kolle, O., Rebmann, C., 2007. EddySoft – Documentation of a software package to acquire and process eddy covariance data. Max Plank-Inst. für Biochem. - Tech. Rep. 10.

Langworthy, A.D., Rawnsley, R.P., Freeman, M.J., Waller, P.A., Corkrey, R., Pembleton, K.G., Harrison, M.T., Lane, P.A., Henry, D.A., 2020. Can irrigating more frequently mitigate detrimental heat wave effects on perennial ryegrass growth and persistence? Agric. For. Meteor. 291. https://doi.org/10.1016/j.agrformet.2020.108074.

Li, J., Tam, C.Y., Tai, A.P.K., Lau, N.C., 2021. Vegetation-heatwave correlations and contrasting energy exchange responses of different vegetation types to summer heatwaves in the Northern Hemisphere during the 1982–2011 period. Agric. For. Meteorol. 296, 108208 https://doi.org/10.1016/j.agrformet.2020.108208.

Li, Y., Guan, K., Peng, B., Franz, T.E., Wardlow, B., Pan, M., 2020. Quantifying irrigation cooling benefits to maize yield in the US Midwest. Glob. Chang. Biol. 26, 3065–3078. https://doi.org/10.1111/gcb.15002.

Lindroth, A., Holst, J., Linderson, M.L., Aurela, M., Biermann, T., Heliasz, M., Chi, J., Ibrom, A., Kolari, P., Klemedtsson, L., Krasnova, A., Laurila, T., Lehner, I., Lohila, A., Mammarella, I., Mölder, M., Löfvenius, M.O., Peichl, M., Pilegaard, K., Soosar, K., Vesala, T., Vestin, P., Weslien, P., Nilsson, M., 2020. Effects of drought and meteorological forcing on carbon and water fluxes in Nordic forests during the dry summer of 2018: drought effects on C&E in boreal forests. Philos. Trans. R. Soc. B Biol. Sci. 375 https://doi.org/10.1098/rstb.2019.0516.

Lloyd, J., Taylor, J.A., 1994. On the temperature dependence of soil respiration. Funct. Ecol. 8, 315. https://doi.org/10.2307/2389824.

Mauder, M., Genzel, S., Fu, J., Kiese, R., Soltani, M., Steinbrecher, R., Zeeman, M., Banerjee, T., De Roo, F., Kunstmann, H., 2018. Evaluation of energy balance closure adjustment methods by independent evapotranspiration estimates from lysimeters and hydrological simulations. Hydrol. Process. 32, 39–50. https://doi.org/10.1002/hyp.11397.

Montagnani, L., Zanotelli, D., Tagliavini, M., Tomelleri, E., 2018. Timescale effects on the environmental control of carbon and water fluxes of an apple orchard. Ecol. Evol. 8, 416–434. https://doi.org/10.1002/ece3.3633.

Niu, S., Luo, Y., Fei, S., Yuan, W., Schimel, D., Law, B.E., Ammann, C., Altaf Arain, M., Arneth, A., Aubinet, M., Barr, A., Beringer, J., Bernhofer, C., Andrew Black, T., Buchmann, N., Cescatti, A., Chen, J., Davis, K.J., Dellwik, E., Desai, A.R., Etzold, S., Francois, L., Gianelle, D., Gielen, B., Goldstein, A., Groenendijk, M., Gu, L., Hanan, N., Helfter, C., Hirano, T., Hollinger, D.Y., Jones, M.B., Kiely, G., Kolb, T.E., Kutsch, W.L., Lafleur, P., Lawrence, D.M., Li, L., Lindroth, A., Litvak, M., Loustau, D., Lund, M., Marek, M., Martin, T.A., Matteucci, G., Migliavacca, M., Montagnani, L., Moors, E., William Munger, J., Noormets, A., Oechel, W., Olejnik, J., U, K.T.P., Pilegaard, K., Rambal, S., Raschi, A., Scott, R.L., Seufert, G., Spano, D., Stoy, P., Sutton, M.A., Varlagin, A., Vesala, T., Weng, E., Wohlfahrt, G., Yang, B., Zhang, Z., Zhou, X., 2012. Thermal optimality of net ecosystem exchange of carbon dioxide and underlying mechanisms. N. Phytol. 194, 775–783. https://doi.org/10.1111/j.1469-8137.2012.04095.x.

Olivares-Soto, H., Bastías, R.M., Calderón-Orellana, A., López, M.D., 2020. Sunburn control by nets differentially affects the antioxidant properties of fruit peel in 'Gala' and 'Fuji' apples. Hortic. Environ. Biotechnol. 61, 241–254. https://doi.org/10.1007/s13580-020-00226-w.

Perkins, S.E., 2015. A review on the scientific understanding of heatwaves – Their measurement, driving mechanisms, and changes at the global scale. Atmos. Res. 164–165, 242–267. https://doi.org/10.1016/j.atmosres.2015.05.014.

Perkins, S.E., Alexander, L.V., 2013. On the measurement of heat waves. J. Clim. 26, 4500–4517. https://doi.org/10.1175/JCLI-D-12-00383.1.

Reich, P.B., Hobbie, S.E., Lee, T., Ellsworth, D.S., West, J.B., Tilman, D., Knops, J.M.H., Naeem, S., Trost, J., 2006. Nitrogen limitation constrains sustainability of ecosystem response to CO_2. Nature 440, 922–925. https://doi.org/10.1038/nature04486.

Reichstein, M., Bahn, M., Ciais, P., Frank, D., Mahecha, M.D., Seneviratne, S.I., Zscheischler, J., Beer, C., Buchmann, N., Frank, D.C., Papale, D., Rammig, A., Smith, P., Thonicke, K., Van Der Velde, M., Vicca, S., Walz, A., Wattenbach, M., 2013. Climate extremes and the carbon cycle. Nature 500, 287–295. https://doi.org/10.1038/nature12350.

Reichstein, M., Falge, E., Baldocchi, D., Papale, D., Aubinet, M., Berbigier, P., Bernhofer, C., Buchmann, N., Gilmanov, T., Granier, A., Grünwald, T., Havránková, K., Ilvesniemi, H., Janous, D., Knohl, A., Laurila, T., Lohila, A., Loustau, D., Matteucci, G., Meyers, T., Miglietta, F., Ourcival, J.M., Pumpanen, J., Rambal, S., Rotenberg, E., Sanz, M., Tenhunen, J., Seufert, G., Vaccari, F., Vesala, T., Yakir, D., Valentini, R., 2005. On the separation of net ecosystem exchange into assimilation and ecosystem respiration: review and improved algorithm. Glob. Chang. Biol. 11, 1424–1439. https://doi.org/10.1111/j.1365-2486.2005.001002.x.

Rita, A., Camarero, J.J., Nolè, A., Borghetti, M., Brunetti, M., Pergola, N., Serio, C., Vicente-Serrano, S.M., Tramutoli, V., Ripullone, F., 2020. The impact of drought spells on forests depends on site conditions: the case of 2017 summer heat wave in southern Europe. Glob. Chang. Biol. 26, 851–863. https://doi.org/10.1111/gcb.14825.

Ruehr, N.K., Gast, A., Weber, C., Daub, B., Arneth, A., 2015. Water availability as dominant control of heat stress responses in two contrasting tree species. Tree Physiol. 36, 164–178. https://doi.org/10.1093/treephys/tpv102.

Scandellari, F., Zanotelli, D., Ceccon, C., Bolognesi, M., Montagnani, L., Cassol, P., Melo, G.W., Tagliavini, M., 2015. Enhancing prediction accuracy of soil respiration in an apple orchard by integrating photosynthetic activity into a temperature-related model. Eur. J. Soil Biol. 70, 77–87. https://doi.org/10.1016/j.ejsobi.2015.07.006.

Schrader, L.E., 2011. Scientific basis of a unique formulation for reducing sunburn of fruits. HortScience 46, 6–11. https://doi.org/10.21273/hortsci.46.1.6.

Seneviratne, S.I., Corti, T., Davin, E.L., Hirschi, M., Jaeger, E.B., Lehner, I., Orlowsky, B., Teuling, A.J., 2010. Investigating soil moisture-climate interactions in a changing climate: a review. Earth-Sci. Rev. 99, 125–161. https://doi.org/10.1016/j.earscirev.2010.02.004.

Solomakhin, A., Blanke, M., 2010. The microclimate under coloured hailnets affects leaf and fruit temperature, leaf anatomy, vegetative and reproductive growth as well as fruit colouration in apple. Ann. Appl. Biol. 156, 121–136. https://doi.org/10.1111/j.1744-7348.2009.00372.x.

Sousa, P.M., Barriopedro, D., García-Herrera, R., Ordóñez, C., Soares, P.M.M., Trigo, R. M., 2020. Distinct influences of large-scale circulation and regional feedbacks in two exceptional 2019 European heatwaves. Commun. Earth Environ. 1, 1–13. https://doi.org/10.1038/s43247-020-00048-9.

Stéfanon, M., Drobinski, P., D'Andrea, F., Lebeaupin-Brossier, C., Bastin, S., 2014. Soil moisture-temperature feedbacks at meso-scale during summer heat waves over Western Europe. Clim. Dyn. 42, 1309–1324. https://doi.org/10.1007/s00382-013-1794-9.

Teskey, R., Wertin, T., Bauweraerts, I., Ameye, M., McGuire, M.A., Steppe, K., 2015. Responses of tree species to heat waves and extreme heat events. Plant Cell Environ. 38, 1699–1712. https://doi.org/10.1111/pce.12417.

Teuling, A.J., Seneviratne, S.I., Stöckli, R., Reichstein, M., Moors, E., Ciais, P., Luyssaert, S., Van Den Hurk, B., Ammann, C., Bernhofer, C., Dellwik, E., Gianelle, D., Gielen, B., Grünwald, T., Klumpp, K., Montagnani, L., Moureaux, C., Sottocornola, M., Wohlfahrt, G., 2010. Contrasting response of European forest and grassland energy exchange to heatwaves. Nat. Geosci. 3, 722–727. https://doi.org/10.1038/ngeo950.

Thiery, W., Davin, E.L., Lawrence, D.M., Hirsch, A.L., Hauser, M., Seneviratne, S.I., 2017. Present-day irrigation mitigates heat extremes. J. Geophys. Res. 122, 1403–1422. https://doi.org/10.1002/2016JD025740.

Thiery, W., Visser, A.J., Fischer, E.M., Hauser, M., Hirsch, A.L., Lawrence, D.M., Lejeune, Q., Davin, E.L., Seneviratne, S.I., 2020. Warming of hot extremes alleviated by expanding irrigation. Nat. Commun. 11, 1–7. https://doi.org/10.1038/s41467-019-14075-4.

Twine, T.E., Kustas, W.P., Norman, J.M., Cook, D.R., Houser, P.R., Meyers, T.P., Prueger, J.H., Wesley, M.L., 2000. Correcting eddy covariance flux underestimates over grassland. Agric. For. Meteorol. 103, 279–300. https://doi.org/10.1016/S0168-1923(00)00123-4.

Von Buttlar, J., Zscheischler, J., Rammig, A., Sippel, S., Reichstein, M., Knohl, A., Jung, M., Menzer, O., Altaf Arain, M., Buchmann, N., Cescatti, A., Gianelle, D., Kiely, G., Law, B.E., Magliulo, V., Margolis, H., McCaughey, H., Merbold, L., Migliavacca, M., Montagnani, L., Oechel, W., Pavelka, M., Peichl, M., Rambal, S., Raschi, A., Scott, R.L., Vaccari, F.P., Van Gorsel, E., Varlagin, A., Wohlfahrt, G., Mahecha, M.D., 2018. Impacts of droughts and extreme-temperature events on gross primary production and ecosystem respiration: a systematic assessment across ecosystems and climate zones. Biogeosciences 15, 1293–1318. https://doi.org/10.5194/bg-15-1293-2018.

Wand, S.J.E., Steyn, W.J., Theron, K.I., 2008. Vulnerability and impact of climate change on pear production in South Africa. Acta Hortic. 800 PART 1, 263–271. https://doi.org/10.17660/actahortic.2008.800.31.

Wang, D., Heckathorn, S.A., Mainali, K., Tripathee, R., 2016. Timing effects of heat-stress on plant ecophysiological characteristics and growth. Front. Plant Sci. 7, 1–11. https://doi.org/10.3389/fpls.2016.01629.

Wohlfahrt, G., Gu, L., 2015. The many meanings of gross photosynthesis and their implication for photosynthesis research from leaf to globe. Plant Cell Environ. 38, 2500–2507. https://doi.org/10.1111/pce.12569.

Wohlfahrt, G., Haslwanter, A., Hörtnagl, L., Jasoni, R.L., Fenstermaker, L.F., Arnone, J. A., Hammerle, A., 2009. On the consequences of the energy imbalance for calculating surface conductance to water vapour. Agric. For. Meteorol. 149, 1556–1559. https://doi.org/10.1016/j.agrformet.2009.03.015.

Xu, H., Xiao, J., Zhang, Z., 2020. Heatwave effects on gross primary production of northern mid-latitude ecosystems. Environ. Res. Lett. 15, 074027 https://doi.org/10.1088/1748-9326/ab8760.

Yuri, J.A., Neira, A., Fuentes, M., Sáez, B., Razmilic, I., 2019. A new sunburned apple category browning under conventional and organic management: phenolic compounds and antioxidant capacity in cold storage. J. Appl. Bot. Food Qual. 92, 288–297. https://doi.org/10.5073/JABFQ.2019.092.040.

Yuri, J.A., Neira, A., Quilodran, A., Razmilic, I., Motomura, Y., Torres, C., Palomo, I., 2010. Sunburn on apples is associated with increases in phenolic compounds and antioxidant activity as a function of the cultivar and areas of the fruit. [WWW Document]. J. Food, Agric. Environ. URLhttps://www.cabdirect.org/cabdirect/abstract/20113031051 (Accessed 17 January 2021).

Zanotelli, D., Montagnani, L., Andreotti, C., Tagliavini, M., 2019. Evapotranspiration and crop coefficient patterns of an apple orchard in a sub-humid environment. Agric. Water Manag. 226, 105756 https://doi.org/10.1016/j.agwat.2019.105756.

Zanotelli, D., Montagnani, L., Manca, G., Scandellari, F., Tagliavini, M., 2015. Net ecosystem carbon balance of an apple orchard. Eur. J. Agron. 63, 97–104. https://doi.org/10.1016/j.eja.2014.12.002.

Zanotelli, D., Montagnani, L., Manca, G., Tagliavini, M., 2013. Net primary productivity, allocation pattern and carbon use efficiency in an apple orchard assessed by integrating eddy covariance, biometric and continuous soil chamber measurements. Biogeosciences 10, 3089–3108. https://doi.org/10.5194/bg-10-3089-2013.